Chemistry of Riming: The Retention of Organic and Inorganic Atmospheric Trace Constituents

Alexander Jost[1,2], Miklós Szakáll[1], Karoline Diehl[1], Subir K. Mitra[2], and Stephan Borrmann[1,2]

[1]Institute for Atmospheric Physics, University of Mainz, 55099 Mainz, Germany
[2]Particle Chemistry Department, Max Planck Institute for Chemistry, 55218 Mainz, Germany

Correspondence to: M. Szakáll (szakall@uni-mainz.de)

Abstract. During free fall in clouds ice hydrometeors such as snowflakes and ice particles grow effectively by riming, i.e., the accretion of supercooled droplets. Volatile atmospheric trace constituents dissolved in the supercooled droplets may remain in ice during freezing or may be released back to the gas phase. This process is quantified by retention coefficients. Once in the ice phase the trace constituents may be vertically redistributed by scavenging and subsequent precipitation or by evaporation of these ice hydrometeors at high altitudes. Retention coefficients of the most dominant carboxylic acids and aldehydes found in cloud water were investigated in the Mainz vertical wind tunnel under dry growth (surface temperature $< 0\,^\circ\mathrm{C}$) riming conditions which are typically prevailing in the mixed phase zone of convective clouds (i.e., temperatures from -16 to $-7\,^\circ\mathrm{C}$ and a liquid water content of $0.9 \pm 0.2\,\mathrm{g\,m^{-3}}$). The mean retention coefficients of formic and acetic acids are found to be 0.68 ± 0.09 and 0.63 ± 0.19. Oxalic and malonic acids as well as formaldehyde show mean retention coefficients of 0.97 ± 0.06, 0.98 ± 0.08 and 0.97 ± 0.11, respectively. Application of a semi-empirical model on the present and earlier wind tunnel measurements reveals that retention coefficients can be well interpreted by the effective Henry's law constant accounting for solubility and dissociation. A parameterization for the retention coefficients has been derived for substances whose aqueous phase kinetics are fast compared to mass transport timescales. For other cases, the semi-empirical model in combination with a kinetic approach is suited to determine the retention coefficients. These may be implemented in high resolution cloud models.

1 Introduction

Riming is an important process leading to the growth of glaciated hydrometeors (e.g., ice particles, snowflakes, graupel grains and hail stones): supercooled liquid droplets collide with frozen drops or ice crystals and freeze subsequently (Pruppacher and Klett, 2010). Hence, it affects the formation of precipitation sized ice particles. During riming soluble species present in the liquid phase could be scavenged, i.e., removed from the atmosphere by precipitation, if they remain in the ice phase during freezing. If they are not removed by precipitation, they may be carried aloft and released upon detrainment and evaporation at higher altitudes e.g. in anvil outflows. Thus, retention during riming in the mixed-phase zone of cumulonimbus clouds and mesoscale convective systems is crucial for the vertical redistribution of trace substances. How much of the species initially dissolved in the supercooled liquid droplets is retained in the final glaciated hydrometeor can be quantified by the so-called "retention coefficient", which assumes percentages or values between 0 and 1. This retention is dependent on chemical properties

such as solubility and dissociation (effective Henry's law constant H^*) but is also affected by physical factors such as droplet sizes, liquid water content, temperature, and ventilation. Ventilation characterizes the enhancement of heat and mass transfer due to flow around the collecting falling hydrometeor. Species with high values of H^* are expected to have 100% retention. For substances with lower values of H^* physical factors and ambient conditions become more important (Stuart and Jacobson,

5   2003, 2004).

These assumptions were confirmed by wind tunnel studies on inorganic species (von Blohn et al., 2011, 2013). Hydrochloric and nitric acids both characterized by high values of H^* were found to be fully retained in ice (von Blohn et al., 2011). For the substances with intermediate values of H^* such as ammonia, hydrogen peroxide, and sulfur dioxide the mean retention coefficients were found to be 0.92 ± 0.21, 0.64 ± 0.11, and 0.46 ± 0.16, respectively, (von Blohn et al., 2011, 2013). The retention

10   coefficient of the most volatile substance sulfur dioxide was significantly affected by the experimental conditions (von Blohn et al., 2013). Thus, one could expect that between 50 and 100% of inorganic species stay in the ice phase during riming which validates riming as an important process for scavenging of chemicals by the ice phase.

Water-soluble organics in the atmosphere are mainly carboxylic acids and aldehydes. Carboxylic acids are ubiquitous components of the troposphere; their primary sources are anthropogenic and biogenic emissions and photochemical transformations

15   of precursors (Chebbi and Carlier, 1996). These substances were detected in measurable quantities in cloud and rain water, as well as in snow samples; even in polar ice (Chapman et al., 1986; Gunz and Hoffmann, 1990; Andreae et al., 1990; Maupetit and Delmas, 1994; Sempéré and Kawamura, 1994). The most abundant carboxylic acids found in cloud water are formic acid, acetic acid, oxalic acid, malonic acid, and succinic acid (Löflund et al., 2002; van Pinxteren et al., 2005). Especially in remote regions they are responsible for up to 65% of acidity in precipitation (Galloway et al., 1982). But also in urban regions car-

20   boxylic acids may contribute significantly to the free acidity in precipitation (Kawamura et al., 1996). Furthermore, they have a low photochemical reactivity in the atmospheric gas phase (photochemical lifetimes are more than a week), so that important sinks for these organic acids are dry and wet deposition (Chebbi and Carlier, 1996; Warneck, 2000; Warneck and Williams, 2012).

Aldehydes are related to human activities (Granby et al., 1997) and photochemistry (Riedel et al., 1999) and are involved in

25   many atmospheric chemistry processes. Photolysis is the main sink of formaldehyde producing OH_X radicals which contribute to the oxidative capacity of the atmosphere (Cooke et al., 2010). However, as formaldehyde is soluble in water there is a pathway for the redistribution by retention. Measurements of cloud water samples showed that formaldehyde is the dominant aldehyde followed by acetaldehyde and propionaldehyde (van Pinxteren et al., 2005). While in the gas phase the photolysis of formaldehyde produces OH_X radicals, in the aqueous phase the reaction of OH with formaldehyde is one of the main sinks

30   for this radical. In this way formaldehyde is responsible for the depletion of approximately 30% of OH under typical in-cloud conditions (Tilgner et al., 2013). Moreover, the reaction of formaldehyde with OH leads to an appreciable amount of formic acid in the aqueous phase (Adewuyi et al., 1984). Furthermore, the aqueous phase oxidation of $S(IV)$ to $S(VI)$ can be inhibited by the reaction of hydrated formaldehyde with free radicals such as OH (Herrmann et al., 2015).

Convective transport is an important process in the distribution of trace substances in the atmosphere since it rapidly transports

35   atmospheric trace gases and aerosols from the boundary layer to the upper troposphere. There they have generally longer life-

times and are more likely to undergo long-range transport (Barth et al., 2007a). Especially in the tropics convective overshoots can lead to injection of ice particles loaded with retained trace substances even in the lowermost stratosphere (Corti et al., 2008; de Reus et al., 2009). Moreover, the shapes of hydrometeors in-situ observed at high altitudes (up to $14\,km$) often indicate the result of riming (Frey et al., 2011). For global models the choice of the needed convection parameterization scheme has a sub-

5   stantial influence on trace gas distributions in a global model (Tost et al., 2010). There are some studies available in literature which investigate the impact of deep convection on the scavenging and redistribution of trace substances in the troposphere (Mari et al., 2000; Barth et al., 2001, 2007b, a; Salzmann et al., 2007; Long et al., 2010; Leriche et al., 2013; Bela et al., 2016) but almost all emphasized the high uncertainty in their modeling studies arising from the lack of experimentally determined retention coefficients. This is especially true for water-soluble organic substances.

10   In contrast to inorganic substances the values for retention coefficients of organics are almost unknown. The aim of this study is to experimentally determine retention coefficients for lower carboxylic acids and aldehydes (formaldehyde) dominantly present in cloud water samples and place the obtained values into the context of those for inorganic species. Performing the experiments at the Mainz Vertical Wind Tunnel Facility allowed the simulation of conditions similar to those in mixed-phase clouds. A further aim was a comparison with previous studies on retention coefficients and to find a general parameterization

15   for retention coefficients which can be implemented in high resolution cloud models.

2   Experimental

In the present experiments single component systems were investigated so that the chemical properties were mainly determined by the substances themselves. This implies that possible interactions between various species present in the liquid phase are

20   not considered (with the exception of CO_2). As liquid water contents and droplet sizes were nearly constant, the experiments provided insight into the effects of physical factors like temperature dependency, and the influence of ventilation and different collector shapes on the retention coefficients. That is, rime collectors such as snowflakes and ice particles were floated in a vertical air flow at velocities ranging from $2\,m\,s^{-1}$ to $3\,m\,s^{-1}$ (i.e., their terminal settling velocities inside clouds) and at typical temperatures where riming is known to be effectively leading to precipitation, namely from -16 to $-7\,°C$ (Pruppacher

25   and Klett, 2010). Table 1 shows a comparison of the experimental parameters and the ones observed in the real atmosphere. Note that only dry growth conditions were investigated, i.e., the surface temperatures of the rime collectors were below $0\,°C$ during riming. The overall methodology adopted to arrive at real retention coefficients is complex and consists of many steps. Involved are (i) realistic hydrodynamical considerations, (ii) application of ion chromatography close to its detection limits, (iii) inclusion of a concentration tracking tracer, (iv) reduction of gas phase concentrations (see Eq. (1) for the operational

30   mathematical expression of the retention coefficients).

Table 1. Comparison between the experimental parameters and the ones observed in the real atmosphere. Given are ranges of the parameters as well as typical values (not necessarily mean values).

Parameter	Experiment		Observed		References
	Range	Typical value	Range	Typical value	
Temperature [°C]	-16 to -7	-11.5	-15 to -5	-10	1, 2, 3
LWC [g m^{-3}]	0.5 to 1.7	0.9	0.5 to 3	1.0	3, 4, 5
Droplet diameter [μm]	2 to 47	8	2 to 140	15	3, 5, 6
Size graupel (diameter) [mm]	–	8	0.5 to 5	2	3, 7
Terminal velocity graupel [m s^{-1}]	–	3.0	0.5 to 4.0	1.8	3, 7, 8
Size snowflakes (diameter) [mm]	10 to 15	13	2 to 15	5	3, 7, 9, 10
Terminal velocity snowflakes [m s^{-1}]	1.8 to 2.3	2.0	0.5 to 1.5	1.3	3, 7, 9, 10, 11

[1]Fukuta and Takahashi (1999); [2]Long et al. (2010); [3]Pruppacher and Klett (2010); [4]Seinfeld and Pandis (2016); [5]Warneck and Williams (2012); [6]Warneck (2000); [7]Locatelli and Hobbs (1974); [8]Pflaum et al. (1978); [9]Hanesch (1999); [10]Brandes et al. (2007); [11]Brandes et al. (2008)

2.1 The flow conditions in the Mainz vertical wind tunnel

In the Mainz vertical wind tunnel hydrometeors from micrometer to centimeter sizes can be freely floated at their terminal fall velocities in a vertical air stream. Therefore, ventilation, i.e., mass and heat transfer are similar to those in the real atmosphere. Ambient air is continuously sucked through the tunnel by means of two vacuum pumps. To perform experiments in the ice phase, the tunnel air can be cooled down to -30 °C. The air flow is laminar with a residual turbulence intensity below 0.5%. More details about the wind tunnel design and experimental characteristics are given in two review papers, Szakáll et al. (2010) and Diehl et al. (2011).

2.2 Supercooled cloud droplet characteristics

The droplet size distribution in the wind tunnel air stream was measured by a Classical Scattering Aerosol Spectrometer Probe Electronics (CSASPE) which is a special unit designed for the wind tunnel by PMS (Particle Measurement Systems, Inc., Boulder, Co, USA). The instrument is capable of measuring the number distribution of droplets from $2 - 47 \mu$m (diameter) in 15 channels with a constant bin size of 3μm. The cloud of droplets was generated in the lower part of the tunnel by two spraying nozzles (Air atomizing nozzles series 1/4 J, Spraying Systems Deutschland GmbH, Hamburg, Germany) in a way such that clogging by freezing was prevented. The upper panel of Fig. 1 shows the number concentration of the supercooled cloud measured in the experimental section of the wind tunnel where the actual retention measurements were performed (corrected for coincidence effects and dead time losses). The average error due to count statistics for each size bin was 23%. The lower panel of Fig. 1 shows the mass distribution, i.e., the normalized cloud liquid water content per size interval. The mass mean diameter of the produced cloud was $22 \pm 14 \mu$m. An alternative measurement for the LWC was obtained from integral
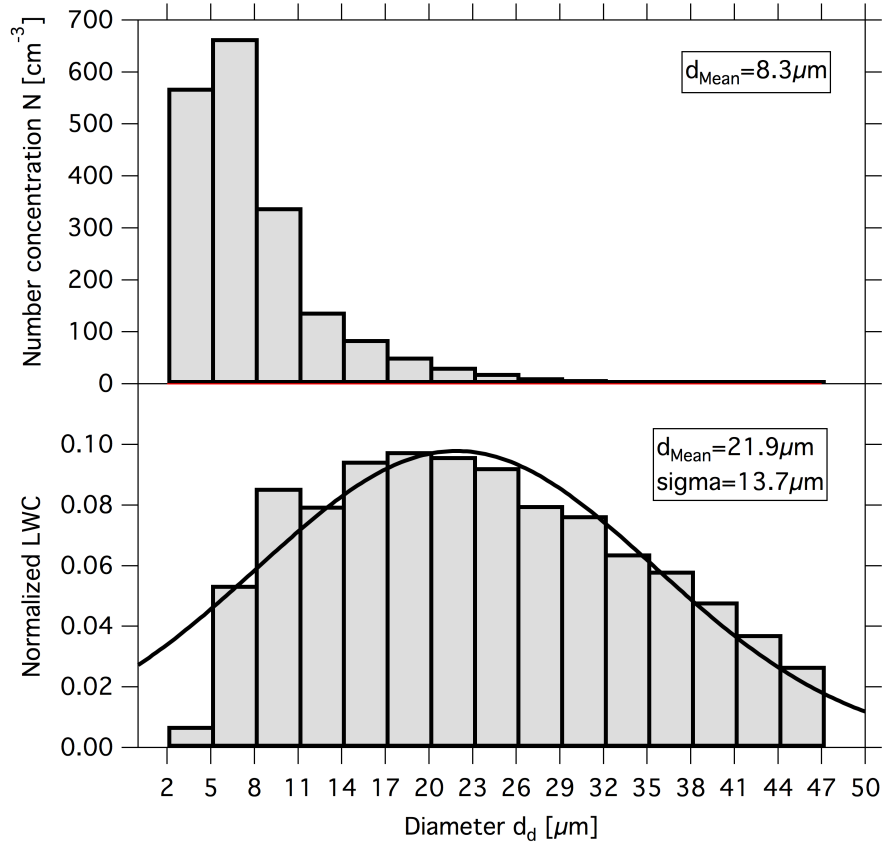
Figure 1. Droplet number (upper panel) and mass (lower panel) distribution of the supercooled cloud generated in the wind tunnel. The average error due to count statistics for the given distributions is 23%.

measurements by means of a dew-point meter (MBW Calibration Ltd., Wettingen, Switzerland, DP3-D/SH) coupled with a 5 m heated pipe. The wind tunnel air containing droplets was sampled through the heated pipe isokinetically. After evaporation the dew point and, thus, the absolute humidity was determined. Afterwards, the dew point of the air without droplets was measured utilizing a droplet separator at the inlet of the heated pipe. By subtracting both absolute humidity values an average LWC of $0.9 \pm 0.2\,\mathrm{g\,m^{-3}}$ was obtained. The averaging refers to at least 100 measurements.

2.3 Liquid phase concentrations

Table 2 summarizes the specifications of the liquid phase (i.e., the supercooled droplets) during the experiments. The second and third columns show concentrations measured in atmospheric cloud water (van Pinxteren et al., 2005) and the concentrations used in the experiments. In order to avoid analysis too close to the detection limit of the ion chromatograph (IC) the concentrations used in the experiments were approximately one order of magnitude higher than those found in cloud water. However, the resulting pH values were in a range which is typically found in cloud water, i.e., from $3.5 - 5.3$ (Löflund et al.,

2002). The solutions, containing a single substance, were prepared out of a high purity grade (see Table 2). Additionally to the trace substance of interest, potassium nitrate (KNO_3) was added as an concentration tracking tracer. Since salts are non-volatile this tracer remained completely in the ice during freezing. The tracer concentration value was used as reference in the retention coefficient calculation to account for processes changing the concentration of the investigated substance. These

5   processes include evaporation of the droplets and dilution of the rime ice due to the pure ice core (see Eq. (1)).

Table 2. Liquid phase concentrations of the investigated substances and corresponding pH. Ambient cloud water concentrations are means of three events (van Pinxteren et al., 2005). The presence of CO_2 ($\approx 400\ \mu\text{mole mole}^{-1}$) was neglected in the pH calculation except for HCHO.

Substance	Cloud concentration [$\mu\text{mol l}^{-1}$]	Experimental concentration [$\mu\text{mol l}^{-1}$]	pH	Label/Purity	Tracer concentration KNO_3 [$\mu\text{mol l}^{-1}$]
Formaldehyde	3.1	100	5.3	Pierce/>97%	30
Formic acid	10.5	65	4.3	Merck/EMSURE	30
Acetic acid	7.2	83	4.5	Merck/EMSURE	30
Oxalic acid	2.0	56	4.3	Fluka/ReagentPlus	30
Malonic acid	0.4	29	4.5	Fluka/ReagentPlus	30

2.4   Experimental procedure

The supercooled solution droplets containing the substance of interest and the tracer were injected into the wind tunnel upstream from the measurement section by the means of two sprayer nozzles which were driven by N_2-gas 99.999%. A specially designed drop separator was installed to avoid high ambient concentrations arising out of the freezing on the tunnel walls of

10   a part of the wide beam of droplets produced by the spraying nozzles. In this way the adsorption of gas molecules of the investigated substances on the rime ice could be neglected. After a duration of approximately $8\,\text{s}$ the droplets reached the measurement section of the wind tunnel where the rime collectors were positioned. Retention is affected by the ability to transfer latent heat to the environment, which is, in turn, given by the shape of the collector and its ventilation properties (including terminal velocity). Therefore, three kinds of rime collectors were investigated: ice particles, snowflakes, and two Teflon-rods

15   (FEP). In addition, during all experiments a liquid nitrogen finger (LN-finger), which consisted of a permanently cooled Teflon test tube (PFA), was used for the determination of the liquid phase concentration of the droplets just before riming. The freezing on the surface of the LN-finger occurred so fast that the retention was 1 and, thus, the original concentration of the rimed droplets could be measured from the deposit by IC.

To avoid a high loss rate and contamination from contacts with the wind tunnel walls the *ice particles* were "captively-floated",

20   i.e., tethered on a thin nylon fiber of $80\ \mu\text{m}$ in diameter. In this manner they were able to move in the airstream without getting lost or become contaminated, but properly simulating the ventilation effect. Another reason for this simplification was the size of the ice particles. For the analysis with IC and the associated minimum injection volume it was necessary to produce a

relatively large ice core when compared to atmospheric ice particles which fall at a terminal velocity of approximately $3\,\mathrm{m\,s^{-1}}$ ($3-4\,\mathrm{mm}$ in diameter (Wang and Kubicek, 2013)). The dimension of such a conical shaped ice particle (produced from IC-grade water) was $8\,\mathrm{mm}$ in diameter. These ice particles would actually have a much higher terminal velocity ($\approx 7.5\,\mathrm{m\,s^{-1}}$; Knight and Heymsfield (1983)), especially because their density was $0.92\,\mathrm{g\,cm^{-3}}$. However, by suspending them, it was pos-

5 sible to ventilate them at a typical vertical velocity of $3\,\mathrm{m\,s^{-1}}$.

The *snowflakes* were produced from dendritic ice crystals (Diehl et al., 1998; Hoog et al., 2007). Snowflakes with diameters between $10\,\mathrm{mm}$ and $15\,\mathrm{mm}$ were positioned on a coarse meshed net. To assure a negligible influence of the net on the rime process it was produced out of a thin nylon fiber with a lattice constant of approximately $8\,\mathrm{mm}$. To account for the correct ventilation, the snowflakes were "quasi-floated", which means that they were floated at an updraft velocity just before they

10 were being lifted from the net. In this manner the velocities were always close to the terminal velocities of the snowflakes. Due to the different sizes and slightly different bulk densities of the snowflakes the terminal velocities varied between $1.8\,\mathrm{m\,s^{-1}}$ and $2.3\,\mathrm{m\,s^{-1}}$.

The *FEP-rods* served as reference since the rimed ice of these collectors was not diluted after melting as in the case of the ice particles and snowflakes. The FEP-collectors were used to measure the retention coefficient at different ventilations. Further,

15 the retention coefficients of these collectors were used for the comparison with previous experimental and theoretical works (Stuart and Jacobson, 2003, 2004).

After a typical exposure time of $10\,\mathrm{min}$ the rimed samples were collected and the meltwater of them were analyzed with IC as described in the next subsection.

2.5   Chemical analysis

20 All five substances were analyzed by ion chromatography using a DIONEX ICS-1000 system (Dionex Corporation) in combination with the software package Chromeleon. Prior to analysis, formaldehyde was oxidized with H_2O_2 to formic acid and analyzed with the same setup as described above (Blank and Finkenbeiner, 1898; Walker, 1964). In order to validate the above method, consistency checks were performed by analyzing exact prepared solutions of known concentrations.

2.6   Calculation of the retention coefficient

25 The retention coefficient was determined by the following ratio:

$$R = \frac{C_{substance}^{sample}/C_{tracer}^{sample}}{C_{substance}^{LN}/C_{tracer}^{LN}}. \tag{1}$$

Here, the numerator describes the ratio of the concentration for the substance of interest in the ice sample $C_{substance}^{sample}$ to the tracer concentration in the ice sample C_{tracer}^{sample}. The denominator describes the same ratio but sampled using liquid nitrogen cooling. With this description, it is not required to account for dilution correction or evaporation correction since these effects

30 change both the substance and the tracer concentration so that the ratio is not altered. This ratio also includes the desorption effect prior to riming since the denominator contains this loss already due to the direct measurement of the liquid phase

concentration. (The retention coefficient is 1 at such deep temperatures.) Therefore, a change in this ratio is solely an effect of the retention of the substance. The error of the liquid phase concentrations is estimated as 4.5% including the instrumental error of the IC and the error of the pipette used for producing the calibration standards for the IC. Taking these errors and applying error propagation on Eq. (1) yields a typical error for the retention coefficients of 9%.

 ## 3   Results and Discussion
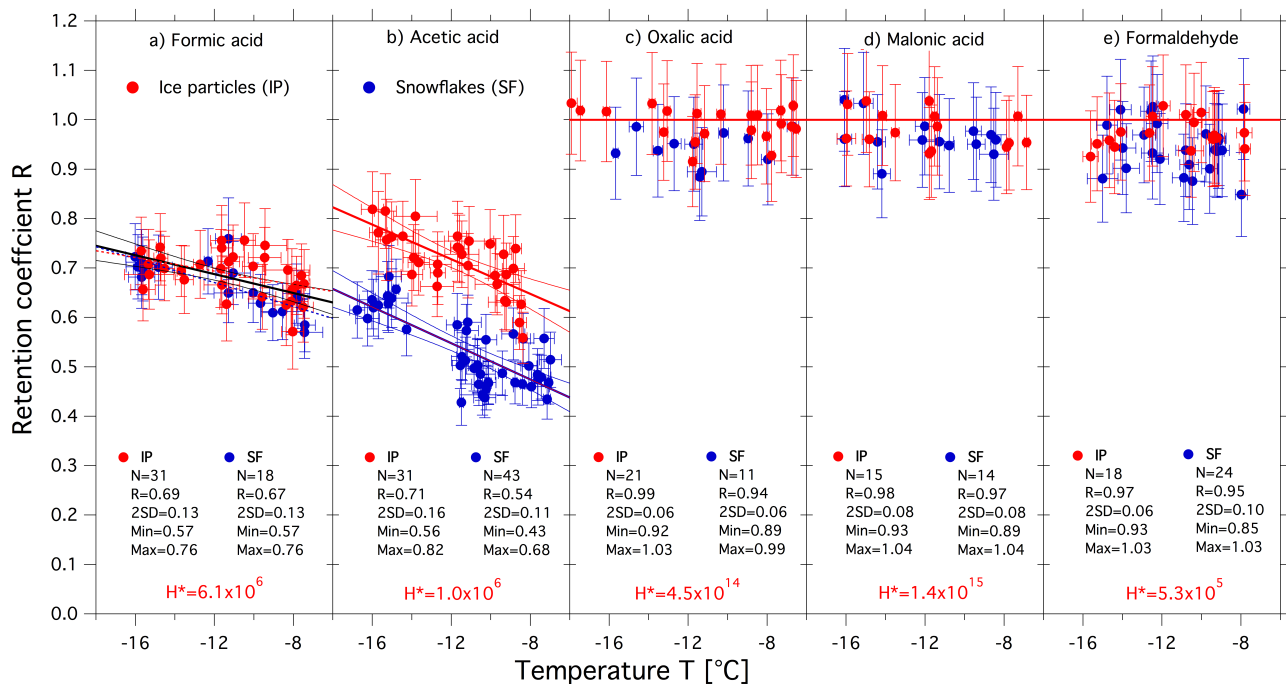
Figure 2. Retention coefficients of all measured substances as function of temperature for different rime collectors. Red symbols: rimed ice particles. Blue symbols: rimed snowflakes. See text for details.

Figure 2 shows the retention coefficients as function of temperature for all investigated organic substances, namely formic acid (a), acetic acid (b), oxalic acid (c), malonic acid (d), and formaldehyde (e). The red symbols depict the rimed ice particles, the blue symbols the rimed snowflakes. Also given in Fig. 2 are the number of data points N and the average retention coefficients R (for formic acid and acetic acid R is the value at $-11.5\,^\circ\mathrm{C}$, for the other substances it is the arithmetic mean including both collector types). The temperature of $-11.5\,^\circ\mathrm{C}$ corresponds to the mean temperature of the measurements and is specified as T_m in the next subsections. In addition to the 95%-error (2SD) and the minimum/maximum-values (labelled as "Min" and "Max"), the dimensionless effective Henry's law constants are shown for the pH of the droplets at $0\,^\circ\mathrm{C}$. Note that all errors in this section correspond to 2SD. In Fig. 2 (a) and (b) the (dashed) red and blue curves represent linear regressions of the retention coefficients of the ice particles and snowflakes, respectively. The black lines in Fig. 2 (a) are the linear regression

as well as the 95% confidence bands of the whole data set, i.e., including all results for ice particles and snowflakes. The red line in panels (c), (d), and, (e) indicates a retention coefficient of 1, or 100%.

3.1 Formic acid

For both rime collectors, the ice particles and the snowflakes, a statistically significant negative temperature dependency (dashed lines in Fig. 2 (a)) was found using a statistical regression test (significance level $\alpha = 0.05$). However, when comparing the linear regressions of both collectors with the 95% confidence bands of the overall regression (solid black lines), the difference of the temperature dependencies of the retention coefficients is negligible. Therefore, the mean retention coefficient is determined by the overall regression which yields $R(T_m) = 0.68 \pm 0.09$. Finally, the retention coefficient of formic acid is only weakly depending on temperature (when considering the error in the observed temperature range) with negligible dependencies on the shape of the collector and the ventilation conditions. The parameterization of the temperature dependency is given in Table 3. The weak temperature dependency might be explained by the intermediate value of H^*. In this range H^* slowly loses its dominant influence which allows the physical factors such as temperature to become more significant. Behind the temperature dependence could be three reasons: First, at higher temperatures ice crystallization inside a freezing droplet proceeds slowly which promotes the segregation process of molecules, i.e., the molecules diffuse more readily into the liquid phase and are not so effectively immobilized by the growing dendrites. This process increases the concentration in the liquid phase and drives the substance into the gas phase. According to Stuart and Jacobson (2006) this is the only factor controlling the solute transport out of the freezing droplet. Second, H^* is lower at higher temperatures which additionally shifts the equilibrium towards the gas phase. Third, at higher temperatures the formation of an ice shell along the surface of the still supercooled liquid proceeds more slowly. Thus, the dissolved substances have more time to escape from the freezing droplet into the gas phase which eventually reduces the retention coefficient.

3.2 Acetic acid

In contrast to formic acid the retention coefficients of acetic acid show a more pronounced temperature dependency. Additionally, a significant dependency of the retention coefficients on the shape of the collectors and the ventilation conditions is evident. The mean retention coefficients of the ice particles and the snowflakes at T_m are 0.72 ± 0.16 and 0.54 ± 0.11, respectively. The corresponding temperature dependencies at the 95% confidence interval of the ice particles and the snowflakes are listed in Table 3. These dependencies can be partially explained by the lower effective Henry's law constant compared to formic acid. Due to the lower H^* the influence of temperature becomes more pronounced. Furthermore, the temperature dependency of H^* of acetic acid is slightly higher compared to that of formic acid which in turn increases the temperature dependency of the retention coefficient. A comparison of the ice particles and the snowflakes shows that the retention coefficient of the snowflakes is on average reduced by 0.18. This decrease might be explained by the combination of the lower value of H^* and a slower heat transfer process for the snowflakes compared to the ice particles which results from the reduced ventilation effect. First, the snowflakes were floated at approximately $2\,\mathrm{m\,s^{-1}}$ while the ice particles were floated at $3\,\mathrm{m\,s^{-1}}$. This difference in the settling velocities arises from the differences in size, bulk density, and shapes of the collectors. Second, the flow through the

branches and around the snowflakes reduces the effective ventilation to the total exposed surface of the snowflakes. Compared to compact sheroidal ice particles this causes slower freezing times of the droplets and as a result acetic acid has more time to escape from the freezing droplets.

3.3 Comparison of the results of formic acid and acetic acid

5   Apparently, the retention coefficients of the snowflakes for formic acid $R(T_m) = 0.67$ and acetic acid $R(T_m) = 0.54$ differ by 0.13. This difference can be explained by taking the mole fractions of the ionic species (formate/acetate) and molecular species (formic acid/acetic acid) into account. H^* depends beside the solubility also strongly on the dissociation of a species which, in turn, is a function of pH. At pH of the formic acid solution droplets ($pH = 4.3$) only 21% of the total dissolved formic acid is present in the molecular form (calculated at $0\,^\circ C$) and the remaining 79% is in the ionic form. In contrast, 10   at $pH = 4.5$ for the acetic acid droplets 64% is present in the molecular form and 36% is in the ionic form. A dissociative substance first has to recombine to the molecular before leaving the droplet and reenter into the gas phase. Thus, acetic acid is three times more present in the molecular form compared to formic acid, which facilitates its escape to the gas phase. As shown below, the kinetics of association (recombination) is fast compared to other timescales involved in the retention process (e.g., those of aqueous phase transport, interfacial transport, gas phase transport of a molecule, and the freezing time). Hence, 15   from the kinetics point of view association has an insignificant impact. However, recombining anions with protons requires energy, which has to be provided by the system. It is argued that overcoming this energy barrier hinders the molecules from recombination. Furthermore, an acetic acid molecule is larger (and rather linearly aligned) than a formic acid molecule which promotes the segregation of acetic acid from ice. This means that the concentration in the liquid part of the freezing droplet increases faster for acetic acid than for formic acid. This effect might lead to the formation of a concentration gradient at the 20   liquid-gas interface forcing the acetic acid molecules to reenter the gas phase.

Comparing the mean retention coefficients ($R(T_m)$) of the ice particles for acetic acid and formic acid shows that they are very close to each other. Due to the stronger temperature dependency the retention coefficients of acetic acid are slightly higher at low temperatures, however, this enhancement is within the measurement uncertainty.

3.4 Dicarboxlyic acids – Oxalic and malonic acids

25   Figures 2 (c) and (d) represent the results of oxalic acid and malonic acid for which H^* are almost 9 orders of magnitude higher compared to the above discussed monocarboxylic acids. This high H^* dominates the retention process (Stuart and Jacobson, 2003) which is also reflected by the experimental results. Application of the statistical regression test on the data of oxalic acid and malonic acid reveals that the retention coefficients for both collectors do not significantly depend on temperature, and the retention coefficients can be given by their average values. The mean retention coefficients of oxalic acid for the ice 30   particles and the snowflakes are 0.99 ± 0.06 and 0.94 ± 0.06, and between the two rime collectors there are no differences. The mean retention coefficients of malonic acid for the ice particles and snowflakes are 1.00 ± 0.08 and 0.96 ± 0.08, respectively. Hence, for both acids the difference between the two rime collectors is negligible. Oxalic acid and malonic acid are strong,

fully dissociated acids at $\mathrm{pH} = 4.3$ and $\mathrm{pH} = 4.5$. This, in combination with their high intrinsic Henry's law constant results in a large H^* that dominates all other environmental parameters influencing the retention process.

3.5 Formaldehyde

Formaldehyde, similarly to the dicarboxylic acids, is almost completely retained in the ice during dry growth riming even for a relative high concentration (c.f., Table 2). From Figure 2 (e) it is obvious that the retention coefficients of the ice particles and the snowflakes are independent of temperature showing high mean retention coefficients of 0.98 ± 0.06 and 0.95 ± 0.10, respectively. As in case of the dicarboxylic acids both values agree within the measurement error. While the retention of the dicarboxylic acids can be explained by the strong dissociation and intrinsic Henry's law constant, formaldehyde is only a weak acid with $pK_a = 13.3$ (Haynes, 2015). Also its intrinsic Henry's law constant is low, comparable to sulfur dioxide or hydrochloric acid. However, it undergoes hydration in aqueous solution forming methanediol (see (R1)) with a hydration constant of $K_{hyd} = k_{R1}/k_{-R1} = 1280$ (at $T = 298$ K; Winkelman et al. (2002)).

$$CH_2O(aq) + H_2O \underset{k_{-R1}}{\overset{k_{R1}}{\rightleftharpoons}} CH_2(OH)_2(aq) \tag{R1}$$

Hence, H^* of formaldehyde does not account for the intrinsic Henry's law constant and dissociation but rather for the intrinsic Henry's law constant and hydration. Especially at low concentrations the $-$ diol form is the favored one so that almost all formaldehyde is present as methanediol and the monomeric formaldehyde is only present in the per mill range (Walker, 1964). Further, at such low concentrations as in the presented experiments all formaldehyde and methanediol are in their monomeric forms (Walker, 1964). Nevertheless, the values for H^* of formaldehyde is rather in an intermediate range, comparable to formic acid and acetic acid, but the retention is 100% within the measurement error. This indicates that it cannot be fully explained by the value of H^*, which only accounts for equilibrium conditions and gives no information on kinetic aspects. If formaldehyde gets dissolved in water its equilibrium between monomeric formaldehyde and methanediol is attained comparatively fast with a rate constant of $k_{R1} = 10.7\,\mathrm{s}^{-1}$ (at $T = 298$ K Winkelman et al. (2002)). However, if the equilibrium is shifted towards monomeric formaldehyde and, thus, the gas phase, methanediol has first to dehydrate with a rate constant which is very low ($k_{-R1} = 8.4 \times 10^{-3}\,\mathrm{s}^{-1}$ at 298 K; Winkelman et al. (2000)). Presumably, the combination of both, the strong hydration of formaldehyde and the low dehydration rate constant are responsible for that high retention coefficient. This means, within the freezing time of a droplet (approximately 1 ms for a ventilated spread $10\ \mu$m droplet) the methanediol dehydrolyzes to a very small extent. Therefore, the dissolved formaldehyde gets almost fully incorporated into the ice phase leading to a retention coefficient close to 1.

4 Application of a semi-empirical model and comparison with previous works

To the best knowledge of the authors, there is no data of retention coefficients for organics available in literature. Therefore, the obtained values are juxtaposed with the corresponding results for inorganic species as measured in earlier studies at the Mainz wind tunnel laboratory (von Blohn et al., 2011, 2013). Two questions are to be answered in this section: i) Is H^* the

Table 3. Retention coefficients of the measured substances, their temperature dependencies, and the effect of ventilation. s.: significant; n.s.: not significant; IP: ice particles; SF: snowflakes. Organic species: present study. Inorganic species: adopted from von Blohn et al. (2011) and von Blohn et al. (2013). HC: high concentration. LC: low concentration.

Substance	Average $R \pm \sigma$	Temperature dependency of R	Ventilation
Formic acid (IP+SF)	0.68 ± 0.05	$R_{tot} = (-0.010 \pm 0.002)T + (0.57 \pm 0.03)$	n.s.
Acetic acid (IP)	0.72 ± 0.08	$R_{ip} = (-0.018 \pm 0.004)T + (0.51 \pm 0.04)$	s.
Acetic acid (SF)	0.54 ± 0.06	$R_{sf} = (-0.018 \pm 0.003)T + (0.33 \pm 0.03)$	s.
Oxalic acid (IP+SF)	0.97 ± 0.03	n.s.	n.s.
Malonic acid (IP+SF)	0.98 ± 0.04	n.s.	n.s.
Formaldehyde (IP+SF)	0.97 ± 0.06	n.s.	n.s.
Sulfur dioxide HC (IP)	0.35 ± 0.08	$R_{ip} = (-0.025 \pm 0.003)T + (0.07 \pm 0.04)$	s.
Sulfur dioxide HC (SF)	0.22 ± 0.05	$R_{sf} = (-0.016 \pm 0.002)T + (0.03 \pm 0.02)$	s.
Sulfur dioxide LC (IP+SF)	0.53 ± 0.09	n.s.	n.s.
Hydrogen peroxide (IP+SF)	0.64 ± 0.14	n.s.	n.s.
Ammonia (IP+SF)	0.92 ± 0.21	n.s.	n.s.
Hydrochloric acid (IP+SF)	0.99 ± 0.03	n.s.	n.s.
Nitric acid (IP+SF)	0.99 ± 0.04	n.s.	n.s.

controlling parameter for both, inorganic and organic substances? ii) Can a reliable parameterization be obtained from such a comparison?

4.1 Model description

A meaningful tool is provided by the semi-empirical model of Stuart and Jacobson (Stuart and Jacobson, 2003, 2004) which relates the experimentally obtained retention coefficients with the so called retention indicator (RI). This is the ratio of the expulsion timescale (τ_{exp}) of a species from the liquid phase to the freezing time (τ_{frz}) of the droplets during riming. In order to find functional dependencies of RI, first a systematic study on the influences of chemical factors, such as the effective Henry's law coefficient, mass accommodation, aqueous diffusivity, gas diffusivity as well as physical factors like temperature, droplet size, ventilation on the retention process were carried out (Stuart and Jacobson, 2003). In a later study, the timescale analysis was extended to dry growth riming accounting for spreading of the droplets' liquid onto the collector's surface and the riming conditions prevailing on a ventilated rimed rod (Stuart and Jacobson, 2004). The most relevant aspects concerning the retention indicator are briefly summarized here (see references for details; e.g., Stuart and Jacobson (2003) and Stuart and Jacobson (2004)).

The expulsion timescale τ_{exp} is the sum of characteristic timescales which are relevant for an individual substance to leave a

water droplet into the gas phase (Schwartz, 1986). Formally the individual timescales are given as

$$\tau_{exp} = \underbrace{\frac{h^2 H^*}{3 D_g \bar{f}}}_{\tau_g} + \underbrace{\frac{4 h H^*}{3 \bar{v} \alpha_m}}_{\tau_i} + \underbrace{\frac{h^2}{D_{aq}}}_{\tau_{aq}} + \tau_r, \tag{2}$$

where $h = 4a/3S^2$ is the spread droplet height, a the droplet radius, S the spreading factor, H^* the effective Henry's law coefficient, $\bar{f}$ the mean gas phase ventilation coefficient (related to the collector's fall speed), D_g the diffusivity of the chemical in air, $\bar{v}$ the thermal velocity of the chemical in air, α the mass accommodation coefficient, and D_{aq} the diffusivity of the chemical in water. The first term on the right hand side of Eq. (2) describes gas phase mass transport (τ_g), the second term the interfacial mass transport (τ_i) and the third term the aqueous phase mass transport (τ_{aq}). Here, a fourth timescale (τ_r) which describes the kinetics of aqueous phase reactions (i.e., association (Seinfeld and Pandis, 2016), dehydration (Winkelman et al., 2000) or reaction with CO_2 (Hannemann, 1995)) is added to the expulsion timescale. This timescale has been neglected in the earlier works (Stuart and Jacobson, 2003, 2004), because acid/base reactions are generally fast compared to the other processes involved. However, as shown below, it becomes important for properly determining the retention coefficients of formaldehyde and ammonia in the presence of carbon dioxide (Hannemann, 1995). The dehydration timescale results from reaction (R1) as it is the inverse first order rate constant k_{-1} of the reverse reaction.

The total freezing time of the droplets is calculated as the sum of the adiabatic and the diabatic freezing time, viz.:

$$\tau_{frz} = \tau_{ad} + \tau_d. \tag{3}$$

During adiabatic freezing no heat exchange with the environment takes place. In the associated time the dendrites penetrate through the supercooled liquid droplet and heat it up to $0\,^\circ C$. Note that in this time only a small fraction of the water mass gets frozen depending on the supercooling of the droplets. It is assumed that shortly after this time ice shell formation is likely to occur. This would inhibit a further removal of the substance from the freezing droplet and, hence, increasing the retention coefficient (Stuart and Jacobson, 2003, 2004, 2006). The diabatic freezing time is determined by the rate of latent heat removal to the underlying rime substrate and the ambient air (Stuart and Jacobson, 2004). The ventilation decreases the diabatic freezing time by increasing the heat removal to the ambient air. Due to the increased ventilation, heat transfer to air dominates over that to the substrate which facilitates ice shell formation. The retention indicator is calculated as

$$RI = \frac{\tau_{exp}}{\tau_{frz}}. \tag{4}$$

If this ratio is much higher than 1 then the substance is assumed to be fully retained in ice. If, in turn, this ratio is much lower than 1, the substance is presumably fully expelled from the freezing droplet. Values for this ratio in an intermediate range are assumed to be directly related to the experimentally obtained retention coefficients (Stuart and Jacobson, 2003, 2004).

All necessary parameters for the calculation of the individual mass transfer timescales (Eq. (2)) together with the references of the values as well as, the limiting timescales, the freezing times (Eq. (3)), the retention indicator (Eq. (4)), and the experimentally obtained retention coefficients for all chemical substances measured in the Mainz wind tunnel laboratory are compiled in Table 4.

4.2 Application of the model to the present and earlier wind tunnel results
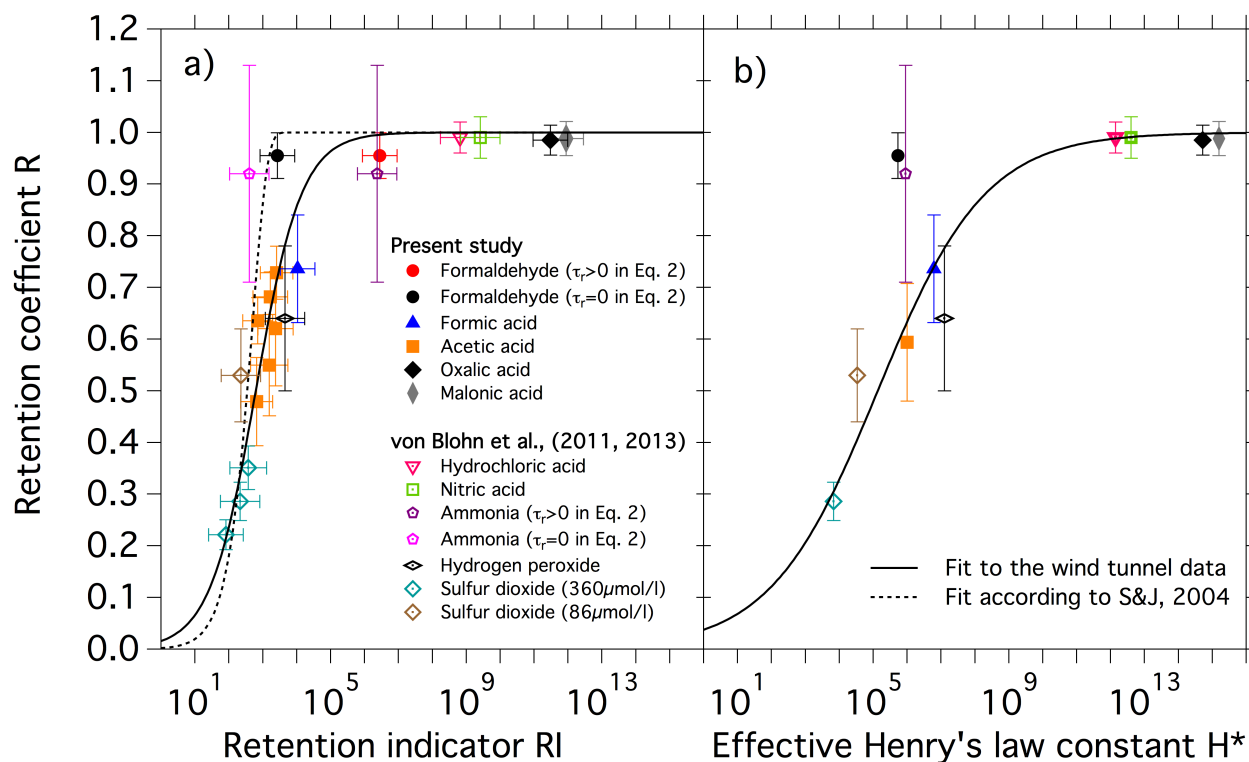
Figure 3. (a): Retention coefficient as function of retention indicator. Filled symbols: organic substances of the present study. Open symbols: wind tunnel data from earlier studies (von Blohn et al., 2011, 2013). The black filled symbol for formaldehyde and the magenta open symbol for ammonia represent values for equilibrium conditions neglecting the aqueous phase kinetics (see text for details). Vertical error bars are measurement uncertainties. Horizontal error bars account for the two limits of adiabatic freezing time and total freezing time of the droplets. Dotted line: fit according to Stuart and Jacobson (Stuart and Jacobson, 2004). Solid line: new fit of the wind tunnel data. **(b)**: Retention coefficients as function of H^*. Symbols according to (a). Solid line: new fit of the wind tunnel data. The H^* values are calculated from literature (see Table 4) at given pH and at $0\,^{\circ}\mathrm{C}$.

In Figure 3 (a) the retention coefficients of organic substances (filled symbols) investigated in the present study as well as the inorganic substances (open symbols) from earlier wind tunnel studies (von Blohn et al., 2011, 2013) are plotted as function of the retention indicator. Note that RI was calculated as the geometric mean of the adiabatic and the total freezing time. The horizontal error bars indicate the two limits of adiabatic freezing and total freezing time of the droplets. In this way it is accounted for ice shell formation which is assumed to be more likely to occur shortly after the adiabatic freezing time (Stuart and Jacobson, 2003, 2004, 2006). The retention coefficient of SO_2 was measured for two different concentrations, one at a high value of $360\,\mu\mathrm{mol\,l^{-1}}$ (HC) and one at a low concentration of $86\,\mu\mathrm{mol\,l^{-1}}$ (LC), which has a retention coefficient of 0.53.

In the HC-case the retention coefficient showed a significant negative temperature trend and, therefore, the retention indicator as well as the retention coefficient were calculated at three different temperatures: $-7; -11; -15\,°C$. The same was done for acetic acid, although in this case it was also distinguished between the different rime collectors in order to account for the ventilation effects. The other substances did not show any significant temperature and ventilation dependencies and, hence, the

5 retention coefficients represent average values. In these cases the retention indicators were calculated at a mean temperature of $-11\,°C$ and at a ventilation corresponding to $3\,m\,s^{-1}$. The retention coefficients used in the intercomparison with the semi-empirical model were obtained from the experiments utilizing FEP-rods as rime collectors. This was done because the freezing time calculations considered the conditions which prevailed on a previously rimed rod. Therefore, the retention coefficients differ slightly from the ones discussed in the previous section. This is especially the case for formic acid, whose retention

10 coefficient is not temperature dependent for the FEP-rods. The heat transfer for these collectors is more efficient compared to the ice particles and the snowflakes since they consisted of a stainless steel core. This caused a faster freezing of the droplets, which counteracted the weak temperature dependency of the retention coefficient for formic acid. A second result originating from the better heat transfer is that the average retention coefficient is slightly higher than in the previously presented results from section 3.1. Consequently, the retention coefficient for formic acid is given as average value and not for three different

15 temperature values. For NH_3 and HCHO RI was calculated for two different expulsion timescales: one neglects the aqueous phase kinetics (i.e. $\tau_r = 0$ in Eq. (2)) while the other one includes it (i.e. $\tau_r > 0$ in Eq. (2)). This is indicated by the magenta open symbol for ammonia and the black filled symbol for formaldehyde for which the aqueous phase kinetics are neglected. In contrast, the values represented by the purple open symbol as well as the red filled symbol include the aqueous phase kinetics. The results for these two substances are discussed in more detail in section 4.3. For the remaining substances RI was calculated

20 including τ_r, however, it is negligible for these substances. That is, τ_r is several orders of magnitude smaller than the other involved timescales. The dotted line in Figure 3 (a) is an exponential function of the following form:

$$R_{SJ} = 1 - \exp(a_5 RI), \tag{5}$$

where $a_5 = -0.002 \pm 0.001$, R_{SJ} is the parameterized retention coefficient, and RI the retention indicator according to Eq. (4) (Stuart and Jacobson, 2004). However, the wind tunnel data suggest a somewhat smoother transition from low to high values.

25 Thus, it is better represented by

$$R_{RI} = \left(1 + (a_6/RI)^{b_6}\right)^{-1}. \tag{6}$$

Here $a_6 = 618 \pm 71$ and $b_6 = 0.64 \pm 0.06$ are fit parameters with 1σ errors. Note that for this parameterization the values for NH3 and HCHO with aqueous phase kinetics are considered. In order to quantify the accuracy of the parameterizations the average absolute error ε is defined as

30 $$\varepsilon = \frac{1}{N} \sum_{i=1}^{N} |R_{SJ,RI}^i - R_{Exp}^i|, \tag{7}$$

where N is the total number of substances i. $R_{SJ,RI}^i$ are the retention coefficients applying Eq. (5) or (6) and R_{Exp}^i are the experimentally obtained values. Utilizing Eqs. (5) and (6) on the data yields $\varepsilon = 0.16$ and $\varepsilon = 0.06$, respectively. Thus, the

presently proposed fit function (Eq. 6) increases the accuracy by a factor of about 2.5 compared to the formerly used exponential function (Eq. 5). This improvement can be attributed to the consistency of the wind tunnel experiments as well as to the larger number of investigated substances. While Eq. (5) is based on five inorganic substances which were measured under different experimental conditions, the wind tunnel data of this study represent results of ten organic and inorganic substances which were measured under very similar experimental conditions.

Since the retention indicator is strongly affected by the effective Henry's law constant (Stuart and Jacobson, 2003) it is worthwhile to investigate the dependency of the measured retention coefficients on H^* (Fig. 3 (b)). The data points represent average values of the retention coefficients of the substances. The fit curve is described by the same functional relationship as in the case of R_{RI}-parameterization (NH_3 and HCHO are excluded as discussed below):

$$R_{H^*} = \left(1 + (a_8/H^*)^{b_8}\right)^{-1}. \tag{8}$$

Here the fit parameters are $a_8 = (1.69 \pm 1.05) \times 10^5$ and $b_8 = 0.26 \pm 0.05$. From Fig. 3 (b) it is obvious that the mean retention coefficients for all investigated acids as well as for H_2O_2 regardless of whether inorganic or organic can be well described solely by H^*. Application of the R_{H^*}-parameterization to the acids and H_2O_2 yields a high accuracy of $\varepsilon = 0.04$. The overall mass transfer timescales (Eq. 2) for the considered substances are mainly controlled by gas phase or interfacial transport (see Table 4). The presence of CO_2 has a negligible effect on the mass transfer for these substances since it is only a weak acid ($pK_a \approx 6.4$) and does not interact with them in the aqueous phase. Even H_2O_2 is not affected by CO_2 because it is more or less independent of pH. Thus, aqueous phase reaction kinetics are negligible for these substances. This makes the retention coefficients a strong function of H^* as previously pointed out in literature (Stuart and Jacobson, 2003, 2004). Furthermore, the experimental conditions of the studies concerning the inorganic substances (von Blohn et al., 2011, 2013) and the present study are very similar. Therefore, the negligible aqueous phase kinetics and the similarity of the experiments are thought to yield such a small value of ε. However, while the R_{RI}-parameterization (Fig. 3 (a)) also accounts for ventilation, temperature, droplet size, and LWC, the R_{H^*}-parameterization (Fig. 3 (b)) only accounts for solubility and dissociation. Nevertheless, to a first order, it describes the mean of the retention coefficients quite well, especially because for most investigated substances temperature and ventilation effects are small. Consequently, the paramerization given in Eq. 8 can be applied to temperatures between $-15\,°C$ and $-7\,°C$ within the corresponding errors.

Note that the most volatile substance depicted in Figure 3 is SO_2. For even more volatile substances the influence of the physical factors might become stronger, probably increasing the error of the R_{H^*}-parameterization. However, the results of SO_2 suggest that the mean of the retention values can be also obtained by the R_{H^*}-parametrization in such cases. While the retention coefficient of SO_2 (LC) showed neither a temperature nor a collector shape (ventilation) dependency, the retention coefficient R for SO_2 (HC) was dependent on both parameters. Moreover, increasing the concentration from $86\,\mu mol\,l^{-1}$ to $360\,\mu mol\,l^{-1}$ led to a decreasing pH from 4.1 to 3.5 resulting in a smaller H^*. Even then the main part of the strong decrease in the retention coefficient from 0.53 to 0.29 could be attributed to the shift in H^* (see Fig. 3 (b)). Therefore, it can be surmised that also for substances which are more volatile than SO_2, H^* is the main factor determining the retention coefficient in the dry growth regime. However, these results show that the retention coefficients for substances which dissociate may be affected

by the pH of the droplets. The effective Henry's law constant H^* combines the dissociation and the intrinsic Henry's law constant. That means, H^* is high and, therefore, the controlling factor when at least one of the two constants has a high value. In such a case the substances are more or less independent of the pH of the droplets because they are either fully dissociated or have a high solubility. On the other hand if both values are low or in an intermediate range, that is, if the substances are not fully dissociated and their solubility is low, they are dependent on pH. Experiments on the concentration dependency of the retention coefficients for HCl and HNO3 showed that their retentions were invariant in a pH range between 2.6 and 3.7. These two substances are fully dissociated for pH > 1, meaning that for higher pH values these acids are expected to show 100 % retention. Furthermore, HNO3 possesses beside the high dissociation constant also a high intrinsic Henry's law constant which suggests a retention of 100 %, even for a pH lower than 1. The same is expected for the two investigated diacarboxylic acids, oxalic acid and malonic acid for low pH values. These two acids have very high intrinsic Henry's law constants and moderate dissociation constants. Thus, their high retention values are mainly caused by the low volatility and not by the dissociation making their retention coefficients more or less independent of pH. This is not the case for the monocarboxylic acids for which the intrinsic Henry's law constants as well as the dissociation constants have moderate values. Hence, the intrinsic Henry's law constant is not the dominating factor making formic acid and acetic acid more sensitively depending on pH, similarly to sulfur dioxide. That means, for a decreasing pH in the droplets the retentions for the monocarboxylic acids presumably decrease too, and vice versa. Finally, the combined value of the equilibrium constants (i.e., H^*) decide to what extend the pH affects the retention. Therefore, the effect of the pH of the droplets on retention is included in the derived parameterizations as is evident from the results of SO_2 and HCl and HNO3.

4.3 Effects of aqueous phase reactions on retention

Conceptually, the R_{H^*}-parameterization is only valid for substances whose aqueous phase kinetics and reactions are negligible. This is not the case for NH_3 and HCHO.

4.3.1 Ammonia

The solubility of NH_3 is increased by several orders of magnitude in the presence of atmospheric CO_2. In the wind tunnel investigations on the retention coefficient of NH_3 the pH of the droplets was measured at consecutive times (von Blohn et al., 2013). Initially the solution had a pH of about 9, which decreased approximately 2 s after the production of the droplets to about 8. Finally the pH of the meltwater from the rimed material was 6.3. This measurement shows that the droplets absorbed CO_2 in the time they were exposed in the wind tunnel (≈ 8 s). However, H^* was calculated at pH 6.3 in Fig. 3 (b) and, thus, accounting already for such an enhancement of the solubility. Nevertheless, the R_{H^*}-parameterization does not reproduce the high retention value of NH_3. In Fig. 3 (a) RI of NH_3 ($RI \approx 400$) was calculated neglecting the aqueous phase kinetics of the CO_2 reaction with NH_3 (see reactions (R2) and (R3) in the text below). According to the R_{RI}-parameterization, R should be about 0.4 which is a deviation much higher than explainable by the measurement error. An experimental study (Hannemann, 1995) on the desorption of NH_3 in the presence of CO_2 from a water drop revealed that the desorption of NH_3 is determined by two different time constants. The first one is governed by the mass transfer equivalent to $\tau_{aq} + \tau_i + \tau_g$ which can be considered

as the inverse of the overall mass transfer rate coefficient k_{mt}^{-1}. However, in the meantime the droplet containing NH_3 absorbs CO_2 gradually which reacts rapidly with OH^- according to the following reaction describing the coupling of NH_3 and CO_2 in alkaline aqueous solution:

$$NH_3(aq) + H_2O \underset{k_{-R2}}{\overset{k_{R2}}{\rightleftharpoons}} NH_4^+ + OH^-, \tag{R2}$$

$$CO_2(aq) + OH^- \underset{k_{-R3}}{\overset{k_{R3}}{\rightleftharpoons}} HCO_3^-. \tag{R3}$$

Initially the system is in equilibrium according to (R2). At the very beginning when the droplets are exposed to ambient air the desorption process is determined by mass transport since the acid/base equilibrium adjusts very fast. In the presence of CO_2 (at alkaline pH) the reaction given by (R3) becomes important and inhibits the reverse reaction (R2). $CO_2(aq)$ reacts fast
10 with OH^- and forms HCO_3^- ($k_{R3} = 2.3 \times 10^3$ s^{-1} at 6.6 °C Wang et al. (2010)). However, the reverse reaction is very slow ($k_{-R3} = 1.4 \times 10^{-5}$ s^{-1} at 6.6 °C Wang et al. (2010)) so that the opportunity of the OH^--ions to recombine with NH_4^+ in order to form the volatile aquatic $NH_3(aq)$ is hindered. Applying also a convective diffusion model including internal circulation of the liquid within the falling drop it was shown (Hannemann, 1995) that the time to completely deplete a drop of 2.88 mm in radius from NH_3 and to reduce CO_2 back to equilibrium conditions would take 1200 s. This timescale is taken into account in
15 the retention indicator calculation as τ_r (Eq. 2). Despite the large differences in the investigated drop sizes it is justified to take that value since desorption is mainly determined by the slow reverse reaction (R3). In other words, the characteristic time of desorption in case of ammonia is controlled by chemical reaction rather than by mass transport.

4.3.2 Formaldehyde

A kinetic effect in the aqueous phase was also observed in the case of HCHO. The high retention coefficient in Fig. 3 (b)
20 cannot be explained by H^* although hydration is included. In Fig. 3 (a) RI for HCHO which only accounts for mass transport (i.e., k_{mt}^{-1}) is given by the red open circle at $RI \approx 3000$. It is in the same range as H_2O_2 and CH_3COOH. However, it shows a retention coefficient of 0.96 which is well above the value predicted by the R_{RI}-parameterization. This indicates that even mass transport effects, like for example mass accommodation, cannot explain the high retention coefficient. Obviously, the overall expulsion timescale is strongly controlled by τ_r which is the rate limiting step in the desorption of HCHO (see
25 Table 4). Consequently, $\tau_r = 1/k_{-R1} = 935.4$ s (k_{-R1} extrapolated to 0 °C) is added to the characteristic timescales for mass transport (Eq. 2). Similarly as in the case of NH_3 the chemical reaction timescale τ_r controls the desorption of HCHO and, therefore, retention. (Here it is not H^* as in cases of negligible aqueous phase kinetics).

The two substances NH_3 and HCHO show how aqueous phase chemical reaction kinetics could influence the retention coeffi-
30 cient. Particularly for such short timescales as the freezing of a 10 μm ventilated spread droplet ($\tau_{frz} \approx 10^{-3}$ s) the recombination/dehydration kinetics become very important for the retention process. On these short timescales this kinetic inhibition of volatilization can be viewed as an increase in solubility. For all other substances for which recombination is fast the retention

can be very well described by mass transport kinetics alone which in dry growth conditions are dominantly determined by H^*. This might not be the case if one considers wet-growth of macroscopic sized hail where not only one parameter dominates the retention of volatile species but rather a combination of the ice-liquid interface supercooling, the liquid water content of the hail, and H^* (Michael and Stuart, 2009). Hence, it is likely that physical factors determining retention such as ventilation,

5 temperature, LWC, and droplet size become more important under wet-growth conditions and H^* loses its dominant role.

5 Conclusions

Wind tunnel experiments were carried out to determine the retention coefficients of lower carboxylic acids and aldehydes during riming. Rime collectors such as snowflakes and ice particles were investigated under typical dry-growth riming conditions, i.e., temperatures from $-16\,\text{to}-7\,^\circ\text{C}$ and a liquid water content of $0.9 \pm 0.2\,\text{g m}^{-3}$. By keeping the liquid water content and

10 the droplet size distribution (mean mass diameter $22 \pm 14\,\mu\text{m}$) nearly constant during each experimental run the measurements provided information about the dependencies of the retention coefficients on ventilation effects (such as heat and mass transfer) and on ambient temperature. The retention coefficients of the measured monocarboxylic acids, formic and acetic acids, showed significant negative temperature dependencies. While the results of formic acid indicated a negligible effect on the ventilation, the results of acetic acid revealed a significant decrease in retention when comparing the ice particles (vertical

15 velocity $w = 3\,\text{m s}^{-1}$) to the snowflakes ($w = 2\,\text{m s}^{-1}$). The measured mean retention coefficients of formic acid and acetic acid were 0.68 ± 0.09 and 0.63 ± 0.19, respectively. Oxalic acid and malonic acid as well as formaldehyde showed retention coefficients of 0.97 ± 0.06, 0.98 ± 0.08, and 0.97 ± 0.11 without a significant temperature and ventilation dependency.

The application of a semi-empirical model (Stuart and Jacobson, 2004) on the present experimental results and on the previously obtained retention coefficients for inorganic substances (von Blohn et al., 2011, 2013) show that retention can be well

20 described by the retention indicator, i.e., the ratio of the sum of kinetic mass transfer timescales to the freezing time of the droplets on the surface of the collector. For those substances for which aqueous phase kinetics (chemical reaction or association) is fast compared to mass transport the mean values of the retention coefficients can be well interpreted using the effective Henry's law constant. The derived functional relationship of retention coefficients on the effective Henry's law constant suggests a high accuracy which makes it a very simple estimation tool for retention coefficients, probably also for substances

25 not investigated so far. Thus, the parameterization can be easily implemented in high resolution cloud models which include retention in the dry-growth riming regime.

However, from the measurements with formaldehyde and ammonia it was found that retention is primarily controlled by aqueous-phase kinetic effects. The retention of formaldehyde is controlled by the dehydation of methanediol. On such short timescales as the freezing of cloud droplets this can be considered as an increase in solubility and, therefore, retention. The

30 retention of ammonia is strongly affected by the kinetics of the reaction of $CO_2(aq)$ with OH^-. Both cases emphasize the importance of accounting for chemical reactions when describing retention. However, modifying the semi-empirical model (Stuart and Jacobson, 2004) by adding appropriate kinetic timescales (e.g., by adding the inverse of dehydration rate) makes it a well suited tool for describing retention coefficients even for such substances for which aqueous-phase kinetics is the limiting

factor. Generally, acid/base reactions are several orders of magnitude faster than mass transport processes. Nonetheless, before applying the R_{H^*}-parameterization it is recommended to first check the recombination/dehydration kinetics of the substance of interest and compare it with the mass transport timescales.

Finally, the work contributes to the improvement of high resolution cloud models which simulate the redistribution of atmo-
5 spheric trace gases. For example, our experiments verify the estimation of the retention coefficients for formic acid and acetic acid applied in Leriche et al. (2013), and Bela et al. (2016). Nevertheless, they underestimated the retention coefficient values of formaldehyde. However, strictly speaking, the present work is only applicable to dry-growth conditions and one component systems in the presence of CO_2. Further experiments which account for more realistic compositions of chemicals in cloud water, for example by measuring retention coefficients of categorized mixtures (tropical, urban, rural, etc.), would give further
10 insight into the process. Moreover, an extension to wet-growth conditions is necessary in order to quantify the retention of trace substances throughout all riming regimes in convective storms.

6   Data availability

Experimental data is freely available upon request to the contact author.

Author contributions. Author contributions: A.J., M.S., K.D., S.K.M., and S.B. designed research; A.J. performed research; A.J., and S.K.M.
15 performed and developed the chemical analysis; A.J., M.S., K.D., S.K.M., and S.B. evaluated the data; A.J., M.S., K.D., S.K.M., and S.B. wrote the paper.

Acknowledgements. This work was supported by the Deutsche Forschungsgemeinschaft under grant MI 483/6-1, as well as by internal funds from the Max-Planck Institute for Chemistry.

Table 4. Input parameters for the determination of the retention indicator and calculated timescales.

Substance	HCHO	HCOOH	CH₃COOH	(COOH)₂	CH₂(COOH)₂	HCl	HNO₃	NH₃	H₂O₂	SO₂ (HC)	SO₂ (LC)
Air temperature, °C	−11	−11	−15 to −7	−11	−11	−11	−11	−11	−11	−15 to −7	−11
Pressure, hPa	1.013×10^3	1.013×10^3	1.013×10^3	1.013×10^3	1.013×10^3	1.013×10^3	1.013×10^3	1.013×10^3	1.013×10^3	1.013×10^3	1.013×10^3
Liquid water content, g m⁻³	0.9	0.9	0.9	0.9	0.9	1.2	1.2	1.2	1.2	1.2	1.2
Mean volume radius of droplets, μm	10	10	10	10	10	13	13	13	13	13	13
Average collector radius, mm	10	10	10	10	10	10	10	10	10	10	10
Wind tunnel air speed, m s⁻¹	3	3	2 to 3	3	3	3	3	3	3	3	3
[1]Spreading factor	1.4	1.4	1.3 to 1.5	1.4	1.4	1.4	1.4	1.4	1.4	1.3 to 1.5	1.4
Height of spread cylinder, μm	6.8	6.8	7.9 to 5.9	6.8	6.8	8.8	8.8	8.8	8.8	10.3 to 7.7	8.8
[2]Surface temperature, °C	−8.7	−8.7	−12.3 to −4.6	−8.7	−8.7	−7.8	−7.8	−7.8	−7.8	−12 to −3.9	−7.8
Growth regime	dry	dry	dry	dry	dry	dry	dry	dry	dry	dry	dry
Concentration, mol l⁻¹	1×10^{-4}	6.5×10^{-5}	8.3×10^{-5}	5.6×10^{-5}	2.9×10^{-5}	4.7×10^{-4}	1.6×10^{-4}	5.9×10^{-5}	2.9×10^{-5}	3.6×10^{-4}	8.6×10^{-5}
[3]pH	5.3	4.3	4.5	4.3	4.5	3.3	3.8	6.4	5.3	3.5	4.1
[4]H^* at given pH (0 °C)	5.3×10^5	6.1×10^6	1.0×10^6	4.5×10^{14}	1.4×10^{15}	1.4×10^{12}	9.4×10^{13}	8.7×10^5	1.6×10^7	5.0×10^3	2.0×10^4
[5]Mass accommodation (0 °C)	0.014	0.047	0.067	0.260	0.307	0.179	0.152	0.202	0.234	0.335	0.335
Thermal velocity in air (0 °C), m s⁻¹	439	355	310	253	236	398	303	583	412	301	301
[6]Diffusivity in air (0 °C), cm² s⁻¹	0.15	0.12	0.10	0.08	0.07	0.14	0.10	0.21	0.14	0.10	0.10
[6]Diffusivity in water (0 °C), cm² s⁻¹	6.9×10^{-6}	7.6×10^{-6}	6.0×10^{-6}	5.3×10^{-6}	4.6×10^{-6}	1.1×10^{-5}	6.8×10^{-6}	1.1×10^{-5}	9.5×10^{-6}	7.3×10^{-6}	7.3×10^{-6}
[7]Ventilation coefficient	31	34	30	32	30	26	38	27	35	32	32
[8]τ_r, s	935.4	1.6×10^{-6}	8.9e − 8	[10]7.0×10^{-7}	[10]1.2×10^{-6}	[11]2.2×10^{-8}	[11]6.3×10^{-8}	[12]1200.0	6.8×10^{-7}	2.9×10^{-7}	2.9×10^{-7}
τ_{aq}, s	6.67e − 2	6.11e − 2	[13]7.70×10^{-2}	8.75×10^{-2}	1.00×10^{-1}	7.24×10^{-2}	1.15×10^{-1}	7.48×10^{-2}	8.22×10^{-2}	1.08×10^{-1}	1.08×10^{-1}
τ_t, s	8.18×10^{-1}	3.31×10^0	[13]4.31×10^{-1}	7.21×10^7	1.96×10^8	2.3×10^5	1.02×10^6	8.99×10^{-2}	1.54×10^0	[13]7.97×10^{-4}	3.96×10^{-3}
τ_g, s	1.66×10^{-2}	2.20×10^{-1}	[13]4.82×10^{-2}	2.95×10^7	1.02×10^8	1.02×10^5	2.8×10^5	4.15×10^{-2}	6.64×10^{-1}	[13]5.64×10^{-4}	2.80×10^{-3}
τ_{exp}, s	9.36×10^2	3.59×10^0	[13]5.56×10^{-1}	1.02×10^8	2.97×10^8	3.34×10^5	1.31×10^6	1.2×10^3	2.28×10^0	[13]1.09×10^{-1}	1.14×10^{-1}
Limiting resistance	τ_r	τ_t	$\tau_t + \tau_g$	$\tau_t + \tau_g$	$\tau_t + \tau_g$	$\tau_t + \tau_g$	$\tau_t + \tau_g$	τ_r	τ_t	τ_{aq}	τ_{aq}
[13]τ_{ad}, s	1.03×10^{-4}	1.03×10^{-4}	1.03×10^{-4}	1.03×10^{-4}	1.03×10^{-4}	1.34×10^{-4}	1.34×10^{-4}	1.34×10^{-4}	1.34×10^{-4}	1.34×10^{-4}	1.34×10^{-4}
[13]τ_d, s	9.93×10^{-4}	9.93×10^{-4}	9.93×10^{-4}	9.93×10^{-4}	9.93×10^{-4}	1.79×10^{-3}	1.79×10^{-3}	1.79×10^{-3}	1.79×10^{-3}	1.79×10^{-3}	1.79×10^{-3}
τ_{frz}, s	1.10×10^{-3}	1.10×10^{-3}	1.10×10^{-3}	1.10×10^{-3}	1.10×10^{-3}	1.93×10^{-3}	1.93×10^{-3}	1.93×10^{-3}	1.93×10^{-3}	1.93×10^{-3}	1.93×10^{-3}
[14]RI	2.79×10^6	1.07×10^4	1.65×10^3	3.02×10^{11}	8.85×10^{11}	6.57×10^8	2.57×10^9	2.36×10^6	4.50×10^3	2.15×10^2	2.25×10^2
[15]R	0.96 ± 0.04	0.74 ± 0.10	0.59 ± 0.11	0.99 ± 0.03	0.99 ± 0.03	0.99 ± 0.03	0.99 ± 0.04	0.92 ± 0.21	0.64 ± 0.14	0.29 ± 0.07	0.53 ± 0.09

1. Inter- and extrapolated from (Brownscombe and Hallett, 1967; Macklin and Payne, 1967, 1969).

2. Calculated for the corresponding LWCs for 3m s⁻¹ (Macklin and Payne, 1967).

3. The presence of CO_2 was neglected except for HCHO and H_2O_2. The pH of NH_3 was measured in the meltwater of the pure rime ice. The pH calculation neglects the 2nd dissociation stage.

4. Calculated at 0 °C and at the corresponding pH (Warneck and Williams (2012); Barret et al. (2011); Johnson et al. (1996); Compernolle and Müller (2014); Marsh and McElroy (1985); Schwartz and White (1981); Hales and Drewes (1979); Maahs (1982)).

5. The mass accommodation coefficients (α at 273K) are taken from a review paper Davidovits et al. (2006) or estimated as described elsewhere (Ervens et al., 2003).

6. The diffusivities in air D_g and in water D_{aq} at 273K have been calculated at 273K (Thibodeaux and Mackay, 2011, p. 78 ff).

7. The convective enhancement of heat and mass transport due to ventilation is calculated for the dimension of the rimed rod using the parameterization of Avila et al. (2001).

8. Calculated from (Seinfeld and Pandis, 2016) unless specified otherwise. Values for k_f and k_r from: (Warneck and Williams (2012); Winkelman et al. (2000, 2002); Kanzaki et al. (2014); Sano and Yasunaga (1973); Eigen et al. (1964)). k_f and k_r specify the forward and reverse reaction rate constants of dissociation/association.

9. Assumed as $1/k_{-1}$ since the mass transport is fast compared to the dehydration rate constant.

10. Sum of first and second dissociation stage timescale: i.e., $\tau_r = \tau_r(1^{st}) + \tau_r(2^{nd})$.

11. k_r assumed to be diffusion controlled $k_r = 5 \times 10^{10}$ l mole⁻¹ s⁻¹.

12. Assumed as the desorption timescale determined by (Hanemann, 1995).

13. Value for 3m s⁻¹ at −11 °C.

14. Calculated for the geometric mean of the adiabatic freezing time τ_{ad} and the total freezing time τ_{frz} as ice shell formation is more likely to occur shortly after the adiabatic freezing time.

15. Note that the values of the present work are arithmetic means of all data points of the FEP-rod collectors (results not shown here).

References

Adewuyi, Y. G., Cho, S.-Y., Tsay, R.-P., and Carmichael, G. R.: Importance of formaldehyde in cloud chemistry, Atmospheric Environment (1967), 18, 2413 – 2420, 1984.

Andreae, M., Talbot, R., Berresheim, H., and Beecher, K.: Precipitation chemistry in central Amazonia, Dry season, Journal of Geophysical Research, 95, 16 987–16 999, 1990.

Avila, E. E., Pereyra, R. G., Castellano, N. E., and Saunders, C. P.: Ventilation coefficients for cylindrical collectors growing by riming as a function of the cloud droplet spectra, Atmospheric Research, 57, 139 – 150, 2001.

Barret, M., Houdier, S., and Domine, F.: Thermodynamics of the Formaldehyde-Water and Formaldehyde-Ice Systems for Atmospheric Applications, Journal of Physical Chemistry A, 115, 307–317, 2011.

Barth, M. C., Stuart, A. L., and Skamarock, W. C.: Numerical simulations of the July 10, 1996, Stratospheric-Tropospheric Experiment: Radiation, Aerosols, and Ozone (STERAO)-Deep Convection experiment storm: Redistribution of soluble tracers, Journal of Geophysical Research, 106, 12 381–12 400, 2001.

Barth, M. C., Kim, S.-W., Skamarock, W. C., Stuart, A. L., Pickering, K. E., and Ott, L. E.: Simulations of the redistribution of formaldehyde, formic acid, and peroxides in the 10 July 1996 Stratospheric-Tropospheric Experiment: Radiation, Aerosols, and Ozone deep convection storm, Journal of Geophysical Research: Atmospheres, 112, 2007a.

Barth, M. C., Kim, S.-W., Wang, C., Pickering, K. E., Ott, L. E., Stenchikov, G., Leriche, M., Cautenet, S., Pinty, J.-P., Barthe, C., Mari, C., Helsdon, J. H., Farley, R. D., Fridlind, A. M., Ackerman, A. S., Spiridonov, V., and Telenta, B.: Cloud-scale model intercomparison of chemical constituent transport in deep convection, Atmospheric Chemistry and Physics, 7, 4709–4731, 2007b.

Bela, M. M., Barth, M. C., Toon, O. B., Fried, A., Homeyer, C. R., Morrison, H., Cummings, K. A., Li, Y., Pickering, K. E., Allen, D. J., Yang, Q., Wennberg, P. O., Crounse, J. D., St. Clair, J. M., Teng, A. P., O'Sullivan, D., Huey, L. G., Chen, D., Liu, X., Blake, D. R., Blake, N. J., Apel, E. C., Hornbrook, R. S., Flocke, F., Campos, T., and Diskin, G.: Wet scavenging of soluble gases in DC3 deep convective storms using WRF-Chem simulations and aircraft observations, Journal of Geophysical Research: Atmospheres, 121, 2016.

Blank, O. and Finkenbeiner, H.: Üeber eine neue Methode zur quantitativen Bestimmung von Formaldehyd, Berichte der deutschen chemischen Gesellschaft, 31, 2979–2981, 1898.

Brandes, E. A., Ikeda, K., Zhang, G., Schönhuber, M., and Rasmussen, R. M.: A Statistical and Physical Description of Hydrometeor Distributions in Colorado Snowstorms Using a Video Disdrometer, Journal of Applied Meteorology and Climatology, 46, 634–650, 2007.

Brandes, E. A., Ikeda, K., Thompson, G., and Schönhuber, M.: Aggregate Terminal Velocity/Temperature Relations, Journal of Applied Meteorology and Climatology, 47, 2729–2736, 2008.

Brownscombe, J. L. and Hallett, J.: Experimental and field studies of precipitation particles formed by the freezing of supercooled water, Quarterly Journal of the Royal Meteorological Society, 93, 455–473, 1967.

Chapman, E., Sklarew, D., , and Flickinger, J.: Organic acids in springtime Wisconsin precipitation samples, Atmospheric Environment, 20, 1717–1725, 1986.

Chebbi, A. and Carlier, P.: Carboxylic acids in the troposphere, occurence, sources, and sinks: a review, Atmospheric Environment, 30, 4233–4249, 1996.

Compernolle, S. and Müller, J.-F.: Henry's law constants of diacids and hydroxy polyacids: recommended values, Atmospheric Chemisty and Physics, 14, 2699–2712, 2014.

Cooke, M. C., Utembe, S. R., Carbajo, P. G., Archibald, A. T., Orr-Ewing, A. J., Jenkin, M. E., Derwent, R. G., Lary, D. J., and Shallcross, D. E.: Impacts of formaldehyde photolysis rates on tropospheric chemistry, Atmospheric Science Letters, 11, 33–38, 2010.

Corti, T., Luo, B. P., de Reus, M., Brunner, D., Cairo, F., Mahoney, M. J., Martucci, G., Matthey, R., Mitev, V., dos Santos, F. H., Schiller, C., Shur, G., Sitnikov, N. M., Spelten, N., Vössing, H. J., Borrmann, S., and Peter, T.: Unprecedented evidence for deep convection hydrating the tropical stratosphere, Geophysical Research Letters, 35, 2008.

Davidovits, P., Kolb, C. E., Williams, L. R., Jayne, J. T., and Worsnop, D. R.: Mass Accommodation and Chemical Reactions at Gas/Liquid Interfaces, Chemical Reviews, 106, 1323–1354, 2006.

de Reus, M., Borrmann, S., Bansemer, A., Heymsfield, A. J., Weigel, R., Schiller, C., Mitev, V., Frey, W., Kunkel, D., Kürten, A., Curtius, J., Sitnikov, N. M., Ulanovsky, A., and Ravegnani, F.: Evidence for ice particles in the tropical stratosphere from in-situ measurements, Atmospheric Chemistry and Physics, 9, 6775–6792, 2009.

Diehl, K., Mitra, S., and Pruppacher, H.: A laboratory study on the uptake of HCl, HNO3, and SO2 gas by ice crystals and the effect of these gases on the evaporation rate of the crystals, Atmospheric Research, 47–48, 235 – 244, 1998.

Diehl, K., Mitra, S. K., Szakáll, M., von Blohn, N., Borrmann, S., and Pruppacher, H. R.: The Mainz vertical wind tunnel facility: a review of 25 years of laboratory experiments on cloud physics and chemistry, in: Wind Tunnels: Aerodynamics, Models, and Experiments, edited by Pereira, J. D., chap. 2, pp. 69–92, Nova Science Publishers, Inc., 2011.

Eigen, M., Kruse, W., Maass, G., and Maeyer, L. D.: Rate Constants of Protolytic Reactions in Aqueous Solution, in: Progress in Reaction Kinetics, edited by Porter, G., vol. 2, pp. 285–318, Pergamon Press Ltd., 1964.

Ervens, B., George, C., Williams, J. E., Buxton, G. V., Salmon, G. A., Bydder, M., Wilkinson, F., Dentener, F., Mirabel, P., Wolke, R., and Herrmann, H.: CAPRAM 2.4 (MODAC mechanism): An extended and condensed tropospheric aqueous phase mechanism and its application, Journal of Geophysical Research: Atmospheres, 108, 2003.

Frey, W., Borrmann, S., Kunkel, D., Weigel, R., de Reus, M., Schlager, H., Roiger, A., Voigt, C., Hoor, P., Curtius, J., Krämer, M., Schiller, C., Volk, C. M., Homan, C. D., Fierli, F., Di Donfrancesco, G., Ulanovsky, A., Ravegnani, F., Sitnikov, N. M., Viciani, S., D'Amato, F., Shur, G. N., Belyaev, G. V., Law, K. S., and Cairo, F.: In situ measurements of tropical cloud properties in the West African Monsoon: upper tropospheric ice clouds, Mesoscale Convective System outflow, and subvisual cirrus, Atmospheric Chemistry and Physics, 11, 5569–5590, 2011.

Fukuta, N. and Takahashi, T.: The Growth of Atmospheric Ice Crystals: A Summary of Findings in Vertical Supercooled Cloud Tunnel Studies, Journal of the Atmospheric Sciences, 56, 1963–1979, 1999.

Galloway, J. N., Likens, G. E., Keene, W. C., and Miller, J. M.: The composition of precipitation in remote areas of the world, Journal of Geophysical Research, 87, 8771–8786, 1982.

Granby, K., Christensen, C., and Lohse, C.: Urban and semi-rural observations of carboxylic acids and carbonyls, Atmospheric Environment, 31, 1403–1415, 1997.

Gunz, D. and Hoffmann, M.: Field investigation on the snow chemistry in central and southern California. II. Carbonyls and carboxyl acids, Atmospheric Environment, 16, 969–981, 1990.

Hales, J. M. and Drewes, D. R.: Solubility of ammonia in water at low concentrations, Atmospheric Environment (1967), 13, 1133 – 1147, 1979.

Hanesch, M.: Fall velocity and Shape of Snowflakes, Ph.D. thesis, Swiss Federal Institute of Technology, 1999.

Hannemann, A.: Eine experimentelle und theoretische Untersuchung zu gekoppelten Aufnahme von SO_2, NH_3 und CO_2 in Wassertropfen, Ph.D. thesis, Institute for Physics of the Atmosphere, University of Mainz, Germany, 1995.

Haynes, W. M., ed.: Handbook of Chemistry and Physics, CRC Press, 96 edn., 2015.

Herrmann, H., Schaefer, T., Tilgner, A., Styler, S. A., Weller, C., Teich, M., and Otto, T.: Tropospheric Aqueous-Phase Chemistry: Kinetics, Mechanisms, and Its Coupling to a Changing Gas Phase, Chemical Reviews, 115, 4259–4334, 2015.

Hoog, I., Mitra, S. K., Diehl, K., and Borrmann, S.: Laboratory studies about the interaction of ammonia with ice crystals at temperatures
5   between 0 and 20 °C, Journal of Atmospheric Chemistry, 57, 73–84, 2007.

Johnson, B. J., Betterton, E. A., and Craig, D.: Henry's Law Coefficients of Formic and Acetic Acids, Journal of Atmospheric Chemistry, 24, 113–119, 1996.

Kanzaki, Y., Tokuda, K., and Bruckenstein, S.: Dissociation Rates of Weak Acids Using Sinusoidal Hydrodynamic Modulated Rotating Disk Electrode Employing Koutecky-Levich Equation, Journal of The Electrochemical Society, 161, H770–H779, 2014.

10 Kawamura, K., Steinberg, S., and Kaplan, I. R.: Concentrations of Monocarboxylic and Dicarboxylic Acids and Aldehydes in Southern California Wet Precipitations: Composition of Urban and Non-Urban Samples and Compositional Changes During Scavenging, Atmospheric Environment, 30, 1035–1052, 1996.

Knight, N. C. and Heymsfield, A. J.: Measurement and Interpretation of Hailstone Density and Terminal Velocity, Journal of the Atmospheric Sciences, 40, 1510–1516, 1983.

15 Leriche, M., Pinty, J.-P., Mari, C., and Gazen, D.: A cloud chemistry module for the 3-D cloud-resolving mesoscale model Meso-NH with application to idealized cases, Geoscientific Model Development, 6, 1275–1298, 2013.

Locatelli, J. D. and Hobbs, P. V.: Fall speeds and masses of solid precipitation particles, Journal of Geophysical Research, 79, 2185–2197, 1974.

Löflund, M., Kasper-Giebl, A., Schuster, B., Giebl, H., Hitzenberger, R., and Puxbaum, H.: Formic, acetic, oxalic, malonic and succinic acid
20   concentrations and their contribution to organic carbon in cloudwater, Atmospheric Environment, 36, 1553–1558, 2002.

Long, Y., Chaumerliac, N., Deguillaume, L., Leriche, M., and Champeau, F.: Effect of mixed-phase cloud on the chemical budget of trace gases: A modeling approach, Atmospheric Research, 97, 540 – 554, 2010.

Maahs, H. G.: Sulfur-dioxide/water equilibria between 0° and 50 °C. An examination of data at low concentrations, in: Heterogeneous Atmospheric Chemistry, edited by Schryer, D. R., pp. 187–195, American Geophysical Union, 1982.

25 Macklin, W. C. and Payne, G. S.: A theoretical study of the ice accretion process, Quarterly Journal of the Royal Meteorological Society, 93, 195–213, 1967.

Macklin, W. C. and Payne, G. S.: The spreading of accreted droplets, Quarterly Journal of the Royal Meteorological Society, 95, 724–730, 1969.

Mari, C., Jacob, D. J., and Bechtold, P.: Transport and scavenging of soluble gases in a deep convective cloud, Journal of Geophysical
30   Research: Atmospheres, 105, 22 255–22 267, 2000.

Marsh, A. and McElroy, W.: The dissociation constant and Henry's law constant of HCl in aqueous solution, Atmospheric Environment, 19, 1075–1080, 1985.

Maupetit, F. and Delmas, J.: Carboxyl acids in high-elevation glacier snow, Journal of Geophysical Research, 99, 16 491–16 500, 1994.

Michael, R. and Stuart, A. L.: The fate of volatile chemicals during wet growth of a hailstone, Environmental Research Letters, 4, 015 001,
35   2009.

Pflaum, J. C., Martin, J. J., and Pruppacher, H. R.: A wind tunnel investigation of the hydrodynamic behaviour of growing freely falling graupel, Quarterly Journal of the Royal Meteorological Society, 104, 179–187, 1978.

Pruppacher, H. R. and Klett, J. D.: Microphysics of clouds and precipitation, Springer, 2 edn., 2010.

Riedel, K., Weller, R., and Schrems, O.: Variability of formaldehyde in the Antarctic atmosphere, Physical Chemistry and Chemical Physics, 1, 5523–5527, 1999.

Salzmann, M., Lawrence, M. G., Phillips, V. T. J., and Donner, L. J.: Model sensitivity studies regarding the role of the retention coefficient for the scavenging and redistribution of highly soluble trace gases by deep convective cloud systems, Atmospheric Chemistry and Physics, 7, 2027–2045, 2007.

Sano, T. and Yasunaga, T.: Kinetic Studies of Dissociation and Recombination Reaction in Aqueous Solutions of Dicarboxylic Acids by Means of Ultrasonic Absorption Measurements, The Journal of Physical Chemistry, 77, 2031–2038, 1973.

Schwartz, S. E.: Mass transport considerations pertinent to aqueous phase reactions of gases in liquid water clouds, in: Chemistry of Multiphase Atmospheric Systems, edited by Jaeschke, W., vol. 6 of *NATO ASI Series*, pp. 415–472, Springer-Verlag Berlin Heidelberg 1986, 1986.

Schwartz, S. E. and White, W. H.: Solubility equilibria of the nitrogen oxides and oxyacids in dilute aqueous solution, in: Advances in Environmental Sciences and Engeneering, edited by Pfafflin, J. R. and Ziegler, E. N., vol. 4, pp. 1– 45, Gordan and Breach Science Publishers, 1981.

Seinfeld, J. H. and Pandis, S. N.: Atmospheric Chemistry and Physics – From Air Pollution to Climate Change, John Wiley and Sons, Inc., 3 edn., 2016.

Sempéré, R. and Kawamura: Comparative distribution of carboxylic acids and related polar compounds in snow, rain, and aerosols from urban atmosphere, Atmospheric Environment, 28, 449–459, 1994.

Stuart, A. and Jacobson, M.: A timescale investigation of volatile chemical retention during hydrometeor freezing: Nonrime freezing and dry growth riming without spreading, Journal of Geophysical Research, 108, 4178, 2003.

Stuart, A. and Jacobson, M.: Chemical retention during dry growth riming, Journal of Geophysical Research, 109, D07 305, 2004.

Stuart, A. L. and Jacobson, M. Z.: A numerical model of the partitioning of trace chemical solutes during drop freezing, Journal of Atmospheric Chemistry, 53, 13–42, 2006.

Szakáll, M., Diehl, K., Mitra, S. K., and Borrmann, S.: Shapes and oscillations of falling raindrops—a review, Journal of Atmospheric Research, 97, 416–425, 2010.

Thibodeaux, L. J. and Mackay, D., eds.: Handbook of Chemical Mass Transport in the Environment, CRC Press, 2011.

Tilgner, A., Bräuer, P., Wolke, R., and Herrmann, H.: Modelling multiphase chemistry in deliquescent aerosols and clouds using CAPRAM3.0i, Journal of Atmospheric Chemistry, 70, 221–256, 2013.

Tost, H., Lawrence, M. G., Brühl, C., Jöckel, P., Team, T. G., and Team, T. S.-O.-D.: Uncertainties in atmospheric chemistry modelling due to convection parameterisations and subsequent scavenging, Atmospheric Chemistry and Physics, 10, 1931–1951, 2010.

van Pinxteren, D., Plewka, A., Hofmann, D., Müller, K., Kramberger, H., Svrcina, B., Bächmann, K., Jaeschke, W., Mertes, S., Jr., J. C., and Herrmann, H.: Schmücke hill cap cloud and valley stations aerosol characterisation during FEBUKO (II): Organic compounds, Atmospheric Environment, 39, 4305–4320, 2005.

von Blohn, N., Diehl, K., Mitra, S. K., and Borrmann, S.: Wind tunnel experiments on the retention of trace gases during riming: nitric acid, hydrochloric acid, and hydrogen peroxide, Atmospheric Chemisty and Physics, 11, 11 569–11 579, 2011.

von Blohn, N., Diehl, K., Nölscher, A., Jost, A., Mitra, S. K., and Borrmann, S.: The retention of ammonia and sulfur dioxide during riming of ice particles and dendritic snow flakes: laboratory experiments in the Mainz vertical wind tunnel, Journal of Atmospheric Chemistry, 70, 131–150, 2013.

Walker, J.: Formaldehyde, American chemical society monograph series, Reinhold, 1964.

Wang, P. K. and Kubicek, A.: Flow fields of graupel falling in air, Atmospheric Research, 124, 158–169, 2013.

Wang, X., Conway, W., Burns, R., McCann, N., and Maeder, M.: Comprehensive Study of the Hydration and Dehydration Reactions of Carbon Dioxide in Aqueous Solution, The Journal of Physical Chemistry A, 114, 1734–1740, 2010.

Warneck, P.: Chemistry of the Natural Atmosphere, International geophysics series, Academic Press, 2 edn., https://books.google.co.uk/books?id=dm4RAQAAIAAJ, 2000.

Warneck, P. and Williams, J.: The Atmospheric Chemist's Companion, Springer, 2012.

Winkelman, J. G. M., Ottens, M., and Beenackers, A. A. C. M.: The kinetics of the dehydration of methylene glycol, Chemical Engeneering Science, 55, 2065–2071, 2000.

Winkelman, J. G. M., Voorwinde, O. K., Ottens, M., Beenackers, A. A. C. M., and Janssen, L. P. B. M.: Kinetics and chemical equilibrium of the hydration of formaldehyde, Chemical Engeneering Science, 57, 4067–4076, 2002.